

## RESEARCH LETTER

10.1002/2014GL059825

## Key Points:

- Coastal low cloudiness from California to Alaska varies coherently over 63 years
- Variability in cloudiness is organized by sea surface temperature variability
- Links from SST to summer cloudiness appear a few months in advance of the summer

## Supporting Information:

- Readme
- Text S1
- Figure S1
- Figure S2
- Figure S3
- Figure S4

## Correspondence to:

R. E. Schwartz,  
reschwartz@ucsd.edu

## Citation:

Schwartz, R. E., A. Gershunov, S. F. Iacobellis, and D. R. Cayan (2014), North American west coast summer low cloudiness: BROADSCALE VARIABILITY ASSOCIATED WITH SEA SURFACE TEMPERATURE, *Geophys. Res. Lett.*, 41, 3307–3314, doi:10.1002/2014GL059825.

Received 6 MAR 2014

Accepted 15 APR 2014

Accepted article online 21 APR 2014

Published online 5 MAY 2014

# North American west coast summer low cloudiness: BROADSCALE VARIABILITY ASSOCIATED WITH SEA SURFACE TEMPERATURE

Rachel E. Schwartz<sup>1</sup>, Alexander Gershunov<sup>1</sup>, Sam F. Iacobellis<sup>1</sup>, and Daniel R. Cayan<sup>1,2</sup>
<sup>1</sup>Scripps Institution of Oceanography, University of California, San Diego, La Jolla, California, USA, <sup>2</sup>U.S. Geological Survey, La Jolla, California, USA

**Abstract** Six decades of observations at 20 coastal airports, from Alaska to southern California, reveal coherent interannual to interdecadal variation of coastal low cloudiness (CLC) from summer to summer over this broad region. The leading mode of CLC variability represents coherent variation, accounting for nearly 40% of the total CLC variance spanning 1950–2012. This leading mode and the majority of individual airports exhibit decreased low cloudiness from the earlier to the later part of the record. Exploring climatic controls on CLC, we identify North Pacific Sea Surface Temperature anomalies, largely in the form of the Pacific Decadal Oscillation (PDO) as well correlated with, and evidently helping to organize, the coherent patterns of summer coastal cloud variability. Links from the PDO to summer CLC appear a few months in advance of the summer. These associations hold up consistently in interannual and interdecadal frequencies.

## 1. Introduction

Summertime cloud intrusion into the terrestrial west coast of North America impacts human, ecological, and logistical systems. The West Coast's relatively low summer daytime temperatures are partially attributed to the seasonally persistent layer of low clouds. Iacobellis and Cayan [2013] estimate that a fluctuation of  $\pm 20\%$  daily mean cloudiness produces a decrease/increase of surface air temperature of  $\sim 1^\circ\text{C}$  along coastal California. Coastal dwellers accustomed to typically mild summer temperatures are more vulnerable to heat waves than the more heat acclimated interior populations [Gershunov et al., 2011; Guirguis et al., 2014]. Coastal species are protected from summer solar radiation by shading and are provided summer water by fog drip [Williams et al., 2008; Fischer et al., 2009]. Low clouds strongly affect coastal solar electricity production, and better accounting of cloudiness can improve solar energy forecasting [Mathiesen et al., 2012]. Aviation at coastal airports is also strongly affected by coastal low cloudiness (CLC) [Hilliker and Fritsch, 1999].

Low stratiform clouds are a persistent feature of continental west coasts that are characterized by a statically stable lower troposphere [Klein and Hartmann, 1993]. Warm, dry air in the descending branch of the Hadley circulation creates the semipermanent North Pacific High, which reaches farthest poleward in Northern Hemisphere summer. Over the midlatitude near-coastal oceans during summer, subsidence from a thermal circulation driven by the large temperature gradient between warm land and cool oceans results in low-level inversions [Klein and Hartmann, 1993]. Vertical mixing of the cool moist marine air is limited by the capping inversion, and formation of stratiform cloud occurs when the upper part of the atmospheric mixed layer reaches saturation [Lilly, 1968; Pilié et al., 1979]. Negative sea surface temperature (SST) anomalies increase low cloud cover by lowering the temperature of the boundary layer and thus increasing lower tropospheric stability and inversion strength [e.g., Klein and Hartmann, 1993; Johnstone and Dawson, 2010, hereinafter JD10; Eitzen et al., 2011]. Conversely, persistent low-level cloud presence can influence SST by reducing surface downward radiation [e.g., Norris and Leovy, 1994; Kubar et al., 2012]. Additionally, in midlatitude summer, low clouds (as fog and stratus) can form without a capping inversion through climatological-mean warm advection [Klein and Hartmann, 1993; Norris and Leovy, 1994; Norris, 1998a].

While many studies have described the strong inverse relationship between SST and low clouds, these analyses are mostly limited to open ocean basins. For example, the coarse "California Stratus Region" at  $20^\circ$ – $30^\circ\text{N}$  and  $120^\circ$ – $130^\circ\text{W}$  of Klein and Hartmann [1993] is far offshore and south of heavily populated coastal California. Norris et al. [1998] report a Pacific basinwide cloud-SST mode that has large loading along the West Coast, but do not address the coastal signal specifically. Most studies that have focused on

the terrestrial coast, conversely have taken a small regional focus. For example, *Witiw and LaDochy* [2008] and *LaDochy and Witiw* [2012] report decreasing trends in annual dense fog frequency only in the Los Angeles region. JD10 examine large-scale climatological air and sea patterns (including in the form of the Pacific Decadal Oscillation (PDO)) but confine their analyses to fog in the coastal Redwood range of northern California. Field campaigns and satellite studies are rich in spatial and temporal resolution [e.g., *Albrecht et al.*, 1988; *Kubar et al.*, 2012], but lack the record length to elucidate multidecadal variability.

Mechanistically, JD10 reported large-scale SST controls on fog for a limited coastal region of northern California. *Norris* [1998a] reported “consistent” physical relationships between low clouds and SST at “substantially different regions” using five ocean weather stations over the Northern Hemisphere. This mechanistic consistency, along with the broadscale Pacific SST anomalies and associated atmospheric circulation, leads to the underlying issue of the present study—is there a similar SST relationship to low clouds along the West Coast beyond northern California, all the way from southern California to the Alaskan Islands?

With specific emphasis on the coastal margin, a set of particular issues are addressed. How does West Coast low cloudiness vary on interannual and interdecadal time scales over six decades, and what is the spatial pattern of this variability over a wide latitudinal range? Are there decreasing trends in summer low cloudiness along the entire West Coast as observed for California subregions in the latter half of the twentieth century and as inferred in the early twentieth century based on a reconstruction of northern California fog reported by JD10? This investigation, which is based upon a set of multidecade airport cloud observations along western North America and International Comprehensive Ocean-Atmosphere Data Set (ICOADS) SST observations over the North Pacific, uses multivariate statistical techniques, including principal component analysis (PCA) and canonical correlation analysis (CCA).

## 2. Data and Methods

Unless otherwise stated, this study employs coastal low cloudiness (CLC, defined in 2.1), for May through September over 63 years from 1950 to 2012.

### 2.1. Airport Cloud Observations

Hourly cloud cover and base height observations were obtained from the National Climatic Data Center (NCDC) Integrated Surface Data (ISD) data set for 20 airports selected due to their proximity to the coast, long record length, and observational sampling consistency. These data were taken by human observers and since the mid-1990s, the majority is taken by ceilometers, a transition that does not create a discontinuity for stratiform low clouds [*Dai et al.*, 2006; *National Weather Service*, 2010]. The airports are, as shown in Figure 1a (approximately from northwest to southeast): Adak, AK (PADK); Cold Bay, AK (PACD); Kodiak, AK (PADQ); Homer, AK (PAHO); Yakutat, AK (PYAK); Sitka, AK (PSIT); Annette Is, AK (PANT); Tofino, BC (CYAZ); Astoria, OR (KAST); North Bend, OR (KOTH); Arcata, CA (KACV); Oakland, CA (KOAK); San Francisco, CA (KSFO); Monterey, CA (KMRY); Vandenberg AFB, CA (KVGB); Point Mugu, CA (KNTD); Los Angeles, CA (KLAX); Long Beach, CA (KLGB); San Diego, CA (KSAN); and North Island, CA (KNZY).

A low cloud observation is defined as having fractional sky cloud cover of at least 0.75, where the clouds under consideration have base heights at or lower than 1 km, consistent with *Iacobellis and Cayan* [2013]. Monthly low-level cloudiness is a measurement of daytime temporal fraction of low cloud cover and is calculated as the fraction of total low cloud observations at 7, 10, 13, and 16 PST to the number of corresponding valid observations. Summer CLC is the mean of May through September monthly values. These daytime hours were selected for consistently high sampling throughout the record and airports. To avoid biases due to the strong diurnal and intraseasonal variation in the low clouds [*Wood*, 2012], if any one of the four daytime hours had less than 25% valid observations for any summer month, the season was set to missing. Missing summers (up to 10) occurred at nine airports and were replaced with the airport's CLC mean.

Low clouds dominate the total cloudiness in the study region (Figure 1b). Two Alaskan airports, PAHO and PANT, have summer low cloud fraction less than 0.50, but results were insensitive to the exclusion of these two airports. To provide a sense of the wide ranging magnitude and variability of CLC (Figure 1b), station mean CLC ranges from 83.8% (PADK) to 13.5% (PAHO) and station standard deviations range from 10.5% (PYAK) to 3.7% (KSFO).

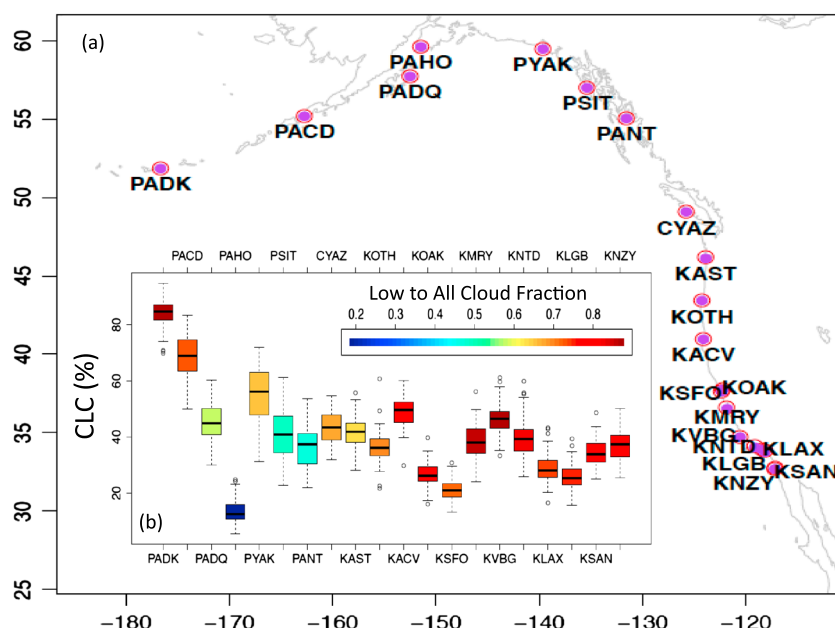


**Figure 1.** (a) Map indicating the 20 coastal airports used. (b) Median, quartiles, and 1.5 times the interquartile range of 1950–2012 CLC denoted by thick line, box, and whiskers, respectively. Color shows the mean fraction of low cloud to all cloud heights.

## 2.2. ICOADS SST

We utilize the  $2^\circ \times 2^\circ$  enhanced monthly mean SST data from the NOAA International Comprehensive Ocean-Atmosphere Data Set (ICOADS release 2.5) [Woodruff *et al.*, 2011] for the North Pacific from  $17.5^\circ\text{N}$  to  $65^\circ\text{N}$ , spanning 1950–2012. Years 2008–2012 are considered preliminary by the ICOADS community. Linear interpolation from neighboring grids was used to fill in grids with missing monthly SST. If a grid cell has missing data for more than 20% of the year from 1950–2012, that cell is excluded.

## 2.3. Climate and Weather Data

Monthly PDO and Niño 3.4 indices were obtained from the University of Washington (<http://jisao.washington.edu/pdo>) and the NOAA Climate Prediction Center (<http://www.cpc.ncep.noaa.gov/data/indices/sstoi>), respectively.

## 2.4. Canonical Correlation Analysis

CCA is a multivariate method employed to identify linear combinations of each of two sets of variables which are maximally correlated with each other. We employ CCA to identify space-time correlated patterns of coastal low cloudiness and North Pacific SST. CCA has been effectively implemented in fields of meteorological and climate variables in diagnostic [Gershunov and Roca, 2004; Guirguis *et al.*, 2014] and predictive capacities [Barnett and Preisendorfer, 1987; Gershunov and Cayan, 2003; Alfaro *et al.*, 2006]. Spatial linear combinations (patterns) of each variable are identified as having time evolutions (canonical correlates; CCs) that are optimally correlated. We use CCA to examine temporally correlated spatial patterns in CLC and SST.

Principal component analysis (PCA) was performed on the summer SST field to reduce the data set dimensionality retained for CCA. The leading PCA spatial mode (empirical orthogonal function (EOF)) highly resembles the PDO pattern [Mantua *et al.*, 1997], and its time series (PC) is correlated with the summer mean PDO index ( $r = 0.94$ ). The leading two PCs explain 20.4 and 11.6% of total SST variance, respectively (not shown). The CCA results reported here are based upon these first two leading SST PCs and CLC at the 20 airports. Experimentation demonstrated that the results reported are robust to inclusion of considerably more SST PCs, up to the point of overfitting when their number exceeds about 15 modes. Thus, the essential large-scale SST variance is captured by the leading two SST PCs and using this truncation yields the most

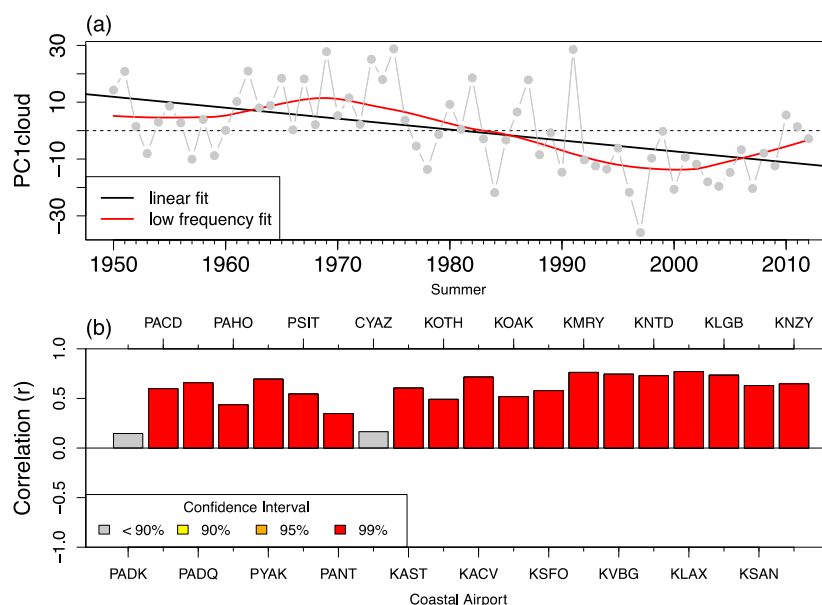


**Figure 2.** Leading CLC (a) PC and (b) empirical orthogonal function (EOF). Linear fit and low-frequency fit of  $PC1_{cloud}$  shown by black and red solid lines, respectively. EOF shown as correlation ( $r$ ) of CLC at each airport to the  $PC1_{cloud}$  time series shown in Figure 2a. Correlations shown in red are significant at a 99% CI.

parsimonious configuration. We focus on the leading CCs, which have the highest correlation between all CC pairs and are referred to as  $CC1_{cloud}$  and  $CC1_{SST}$ , because they describe the large-scale patterns that are germane to the present study. The leading cloud CC, from a CCA version based upon high-pass filtered SST and CLC inputs, is denoted  $CC1_{cloud\_HP}$ .

### 3. Results

#### 3.1. Coherent Variation of Summertime Coastal Low Cloudiness

CLC variability, over the six decade period of record, is coherent along a broad coastal swath of western North America, from southern California to the Alaskan Islands (Figure 2). The leading CLC mode explains 39% of the total CLC variance (Figure 2b) and highlights the coherent nature of coastal low cloud variation with an in-phase relationship for all 20 airports, significant at 99% confidence interval (CI) for all but two airports (CYAZ and PADK). The leading PC ( $PC1_{cloud}$ , Figure 2a) is significantly decreasing over the 1950 to 2012 record for a linear fit, yet  $PC1_{cloud}$  also exhibits considerable interannual and interdecadal variability beyond this decreasing trend.

Consistent with the leading CLC mode, coastal airport locations which experienced decreasing CLC are found along the northern and southern West Coast. The overall mean fractional CLC decline from the first decade (1950–1959) to the last decade (2000–2009) of record is about 5% when averaged over the 19 airports with sufficient nonmissing data for these decades. Significantly decreasing trends occurred over the full record for 12 out of the 20 airports (Figure S1, labeled in blue, in the supporting information). In addition to the full 63 year record, we examine linear trends at each airport for 30 year moving window periods (Figure S1). All airports except for four (KOTH, KOAK, KSFO, and KVBG) in the central West Coast region exhibit 30 year periods of significantly decreasing CLC. Consistently across airport locations, the most decreasing trends occurred near the middle of the record from the late 1960s to early 2000s. Thirty year periods with significantly increasing CLC occurred at five airports, and of these five, for all but CYAZ, periods of increasing CLC occurred early in the record.

#### 3.2. The Role of Sea Surface Temperature

The leading CCA mode exhibits a strong negative relationship between eastern North Pacific SST and CLC along the entire West Coast from San Diego, CA (KSAN) to Cold Bay, AK (PACD) (Figure 3). The time series  $CC1_{SST}$  and  $CC1_{cloud}$  (Figure 3a) representing the temporal evolution of the spatial patterns in SST and CLC

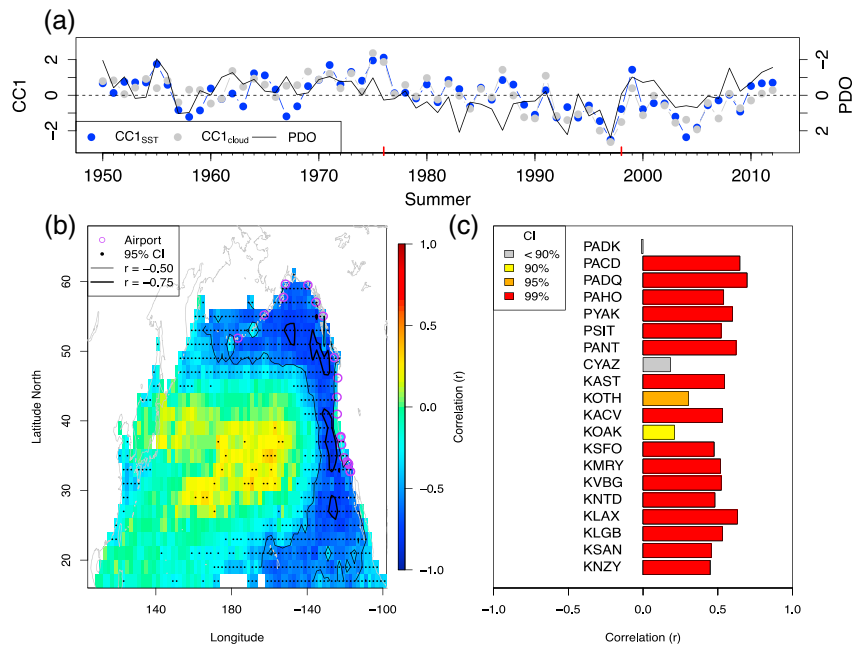


**Figure 3.** (a) CCA leading mode of SST and CLC,  $CC1_{SST}$  (blue),  $CC1_{cloud}$  (gray), summer PDO (black, note axis reversed). Spatial patterns of (b) SST and (c) CLC are displayed as correlations of the time series (Figure 3a) with their respective variable fields at each location. In Figure 3a, red tick marks denote regime shifts in summer PDO as identified by Overland *et al.* [2008]. In Figure 3b, purple circles denote airport locations, black dots denote grid cells with correlations significant at the 95% CI, thin (thick) black contours represent  $r = -0.5$  ( $-0.75$ ). In Figure 3c, red, orange, and yellow bars show correlations significant at the 99%, 95%, and 90% CI, respectively.

(Figure 3b and 3c, respectively) are optimally correlated, at  $r = 0.79$ . Spatially,  $CC1_{cloud}$  represents a coherent in-phase cloud variation at 19 of 20 coastal locations, and represents 28.6% of total CLC variance (Figure 3c).  $CC1_{cloud}$  (Figure 3a gray) and the leading PCA mode of CLC ( $PC1_{cloud}$ , Figure 2a) are correlated at  $r = 0.83$ , confirming that  $CC1_{cloud}$  is a prominent mode of total CLC variability along the entire West Coast besides simply being optimally correlated to SST (as is the method's design).

The time variation of  $CC1_{SST}$  and  $CC1_{cloud}$  (Figure 3a) illustrates the interdecadal nature of the SST-low cloud relationship and clearly indicates that the trend toward decreasing cloudiness is associated with increasing eastern Pacific SST. The broadscale multidecadal increase in eastern Pacific SST (in contrast with central Pacific SST) is consistent with the decreasing trends of CLC at individual West Coast stations described above.  $CC1_{cloud}$  decreases over the 1950 to 2012 record period. Interestingly, it is not the low frequency variation alone that drives the CCA leading mode result. A separate CCA performed on the high-pass filtered fields indicates the CCA leading mode relationship (Figure 3) holds at interannual timescales and  $CC1_{cloud\_HP}$  retains spatial coherency along the West Coast (Figure S2). Thus, highlighting the interannual strength of the SST-low cloud relationship in addition to the interdecadal one.

The leading North Pacific SST pattern associated with CLC variability ( $CC1_{SST}$ ) is correlated moderately with the PDO index (Figure 3a). Thus also,  $CC1_{cloud}$  is related to contemporaneous PDO ( $r = -0.46$ ). The spatial pattern of  $CC1_{SST}$  (Figure 3b) is highly similar to the SST pattern associated with northern California fog reported by JD10 and appears as slightly modified from the PDO pattern. The  $CC1_{SST}$  eastern Pacific signal is more narrowly confined toward the West Coast and is stronger than the out-of-phase central and western Pacific signal of the PDO. El Niño–Southern Oscillation, as represented by the Niño 3.4 SST anomaly, is also correlated with  $CC1_{SST}$ , albeit weakly ( $r = -0.30$ ). To isolate and investigate interannual relationships and, in particular, potential leads and lags between SST and CLC, high-pass filtered  $CC1_{cloud\_HP}$  and high-pass filtered monthly PDO indices ( $PDO_{HP}$ ) are examined (Figure 4). Contemporaneous summer  $CC1_{cloud\_HP}$  and  $PDO_{HP}$  share 23.2% variance ( $r = -0.48$ ). Moreover, an asymmetrical relationship between SST anomalies (represented by monthly  $PDO_{HP}$ ) and CLC (represented by  $CC1_{cloud\_HP}$ ) is revealed by leading versus lagging

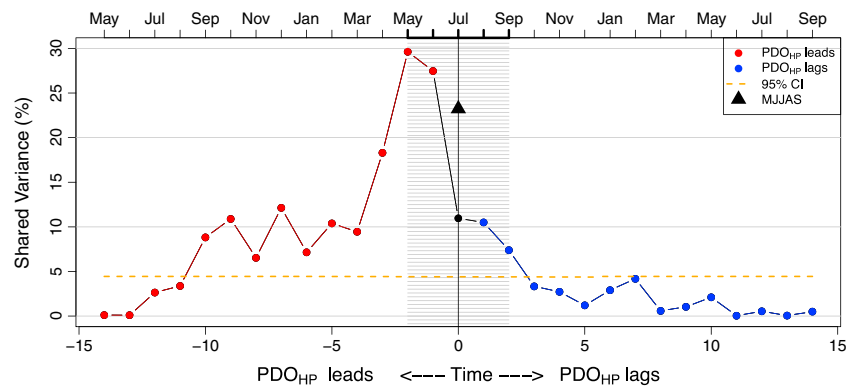


**Figure 4.** Shared variance between summer (gray region)  $CC1_{cloud\_HP}$  and monthly  $PDO_{HP}$ . Months before (after) contemporaneous July are shown in red (blue). Orange dashed line denotes 95% CI. Contemporaneous summer mean shown by triangle.

SST in Figure 4.  $PDO_{SST}$  is significantly correlated to cloudiness for up to 10 months in advance (previous September), yet correlation becomes insignificant for  $PDO$  lagging cloudiness at 3 months (following October) and beyond.

#### 4. Discussion and Conclusions

This paper highlights the interaction between basinwide North Pacific sea surface temperature (SST) variability and coastal low cloudiness (CLC). The anomalous low cloud pattern, closely associated with North Pacific SST, extends beyond the ocean to the terrestrial West Coast margin, stretching from at least Southern California to the Alaskan Islands. This extensive low cloud pattern varies coherently at a wide range of time scales, from summer to summer and decade to decade. The asymmetric SST-leads-cloud correlation indicates that SST patterns drive West Coast low cloud fluctuations. Beginning in the late 1950s, a long period of decreasing CLC associated with increasing eastern North Pacific SST is apparent in  $CC1_{cloud}$ ,  $PC1_{cloud}$  and most individual airport low cloud records.

The extensive CLC structure clearly encompasses multidecadal anomalies in CLC along the California coast [e.g., Johnstone and Dawson, 2010; Witiw and LaDochy, 2008], and the results here reveal a pattern of fluctuations that is organized over much of the North American west coast. Broadly coherent fluctuations of low cloudiness have previously been shown over the open ocean [e.g., Norris and Leovy, 1994], but it is apparent that linked multiyear variability is also operating over the coastal terrestrial margin, in spite of its more complex terrain with inhomogeneous topography, surface heating, and surface moisture. The consistency of our broadscale coastal findings with those of maritime-based analyses and the strong linkage between cloud variability and SST patterns supports the notion that coastal low clouds are in essence an extension of the large-scale marine low-cloud field.

Coastal terrain complexities may explain some of the differences that emerge at the airports beyond their striking coherency. For example, KOTH, KOAK, KSFO, and KVGB are the only coastal locations examined to not show a significantly decreasing 30 year trend in the low cloud record (Figure S1b). While all airports are coastal, local topography, which impacts low-level clouds [Simon, 1977], should have local effects. KSFO is on the bay side of the San Francisco Peninsula, separated from the Pacific coast by coastal topography, for example. PADK and CYAZ are the only two locations both insignificantly represented by the leading  $PC1_{cloud}$  (Figure 2) and  $CC1_{cloud}$  (Figure 3c). That these are the same two locations underrepresented by both the univariate and multivariate (with SST) leading modes of cloud variability actually reiterates that the coherency seen in the other 18 coastal locations is organized by SST. CYAZ is unique among all other locations in that it has as many 30 year periods of increasing as decreasing trends in CLC and exhibits the increasing trends into the end of the record (Figure S1). PADK represents the northwest extremity in the spatial range of the West Coast examined here. PADK may lie beyond the “West Coast” regime and respond to central more than eastern Pacific influence.

Additional evidence and insight into the lower tropospheric structure over the West Coast is provided by seven coastal radiosonde sites. While subsidence inversions are nearly ubiquitous in summer at the two



California sites, inversions are observed less frequently, from about 20% to 40% of afternoons, for the one Washington and four Alaska locations examined. If anything, these atmospheric structure differences revealed by radiosonde data reinforce how surprising the spatial consistency is as quantified by both  $PC1_{cloud}$  (Figure 2) and  $CC1_{cloud}$  (Figure 3). That is, over the broad coastal swath examined, the in-phase SST organization of cloudiness likely occurs for different low cloud types. Not surprisingly, given previous regional results [e.g., Norris, 1998b], this structure includes clouds that predominantly occur under an inversion, but interestingly, it also includes clouds that occur in northern latitudes that quite often are not associated with an inversion. Even given that the climatological mean states of the atmospheric environments differ (e.g., in terms of inversion presence), we see that there is some association between summers of much (little) CLC and more (fewer) inversions (Figure S3). For clouds influenced by an inversion, low SST can help strengthen the inversion from below. Another factor driving inversion strength is atmospheric circulation [e.g., Klein *et al.*, 1995], presumably related to subsidence, advection, and possibly other mechanisms. We do not focus on atmospheric circulation here, but have found (results not shown) that sea level pressure has a less coherent—more regional association with the 20 individual coastal locations than does SST.

Figure 4 suggests possible seasonal predictability of large-scale summertime CLC from previous SST anomaly patterns, as captured by the PDO. Previously, Alfaro *et al.* [2004] demonstrated the predictive capability of spring PDO for subsequent summer (June–July–August) temperatures over California and, in particular, for coastal California. In light of the leading PDO–CLC relationship shown in the present study and estimate of coastal cloudiness' impact on surface temperature by Iacobellis and Cayan [2013], the PDO signal in coastal daytime temperatures found by Alfaro *et al.* [2004] may be accomplished in part through PDO-driven fluctuations in CLC. Splitting the record at the 1976–1977 PDO shift [Mantua and Hare, 2002], to roughly separate the cool and warm PDO phases, we find the asymmetric relationship to hold in both segments of the record, although the 1950–1976 period has a somewhat stronger PDO SST-leading relationship beginning in February (Figure S4). We do not, on the other hand, find a consistently significant relationship between low cloudiness and subsequent SST as others have, e.g., Norris and Leovy [1994] and Kubar *et al.* [2012], but this may be expected given the different regions and time scales of analyses.

The delineation of the large-scale coherent cloud pattern is obscured in its southern reach by the lack of long-term consistent observations. From the broad southward extent of eastern North Pacific SST anomalies and the spatial coherence of stratus based on a shorter record of satellite albedo records [Iacobellis and Cayan, 2013], we expect the pattern to extend along the Pacific coast of Baja California, Mexico. Given the low frequency variability of southeastern Pacific SST [Falvey and Garreaud, 2009] and the persistent coastal South American low clouds [Klein and Hartmann, 1993], an exploration of CLC variability along the west coast of the Americas should be insightful. Additionally, the present analysis likely misses higher-frequency variability [Kubar *et al.*, 2012], as well as possibly more local variability including intraseasonal timing, since the present study is focused on interannual and interdecadal variation in cloudiness averaged over an extended 5 month summer season (May–September).

Over the six decades of record, summer low cloudiness at many coastal locations diminished by more than 5%. This decrease since 1950 may be modest compared to variability and, in particular, compared to an apparent larger decline earlier in the twentieth century inferred by JD10 using a reconstruction of northern California fog. As for the potential of a continuing, long-term reduction of CLC, in recent years the decreasing trend has weakened or even reversed at most coastal locations. This letup is consistent with the upturn beginning in 1998 for both annual fog in coastal Los Angeles [LaDochy and Witiw, 2012] and summer fog in northern California reported by JD10. This CLC resurgence is consistent with the recent tendency for cool SST along the West Coast after the strong 1997–1998 El Niño. Clearly, it is important to determine if the trends in CLC may be affected by anthropogenic factors, but explicit accounting for anthropogenic influence is beyond the scope of the present study.

## References

- Albrecht, B. A., D. A. Randall, and S. Nicholls (1988), Observations of marine stratocumulus during FIRE, *Bull. Am. Meteorol. Soc.*, *69*, 618–626.
- Alfaro, E., A. Gershunov, D. R. Cayan, A. Steinemann, D. W. Pierce, and T. P. Barnett (2004), A method for prediction of California summer air surface temperature, *Eos Trans. AGU*, *85*(51), 553–558.
- Alfaro, E., A. Gershunov, and D. R. Cayan (2006), Prediction of summer maximum and minimum temperature over the Central and Western United States: The role of soil moisture and sea surface temperature, *J. Clim.*, *19*(8), 1407–1421.
- Barnett, T. P., and R. Preisendorfer (1987), Origins and levels of monthly and seasonal forecast skill for United States surface air temperatures determined by canonical correlation analysis, *Mon. Weather Rev.*, *115*, 1825–1850.

## Acknowledgments

We thank NASA for support of RES through Earth and Space Science Fellowship 12-EARTH12F-0080 and California Energy Commission for support of SFI and DRC through agreement 500-10-041. Additional support was provided by the NSF through Climate Education Partners award DUE-1239797 (sandiego.edu/climate). This study contributes to DOI's Southwest Climate Science Center activities and to NOAA's California and Nevada Applications Program award NA11OAR4310150. We thank Alex Tardy, Joel Norris, Nathan Mantua, and an anonymous reviewer for helpful comments. ICOADS data were provided by the NOAA/OAR/ESRL PSD, Boulder, Colorado, USA, from <http://www.esrl.noaa.gov/psd>. Airport cloud observations were obtained from the Global Surface Hourly database at <http://www.ncdc.noaa.gov> operated by the NOAA National Climatic Data Center (NCDC).

The Editor thanks two anonymous reviewers for their assistance in evaluating this paper.

- Dai, A., T. R. Karl, B. Sun, and K. E. Trenberth (2006), Recent trends in cloudiness over the United States: A tale of monitoring inadequacies, *Bull. Am. Meteorol. Soc.*, 87(5), 597–606.
- Eitzen, Z. A., K. M. Xu, and T. Wong (2011), An estimate of low-cloud feedbacks from variations of cloud radiative and physical properties with sea surface temperature on interannual time scales, *J. Clim.*, 24(4), 1106–1121, doi:10.1175/2010JCLI3670.1.
- Falvey, M., and R. D. Garreaud (2009), Regional cooling in a warming world: Recent temperature trends in the southeast Pacific and along the west coast of subtropical South America (1979–2006), *J. Geophys. Res.*, 114, D04102, doi:10.1029/2008JD010519.
- Fischer, D. T., C. J. Still, and A. P. Williams (2009), Significance of summer fog and overcast for drought stress and ecological functioning of coastal California endemic plant species, *J. Biogeogr.*, 36(4), 783–799, doi:10.1111/j.1365-2699.2008.02025.x.
- Gershunov, A., and D. Cayan (2003), Heavy daily precipitation frequency over the contiguous United States: Sources of climatic variability and seasonal predictability, *J. Clim.*, 16(16), 2752–2765.
- Gershunov, A., and R. Roca (2004), Coupling of latent heat flux and the greenhouse effect by large-scale tropical/subtropical dynamics diagnosed in a set of observations and model simulations, *Clim. Dyn.*, 22(2–3), 205–222.
- Gershunov, A., Z. Johnston, H. G. Margolis, and K. Guirguis (2011), The California heat wave 2006 with impacts on statewide medical emergency: A space-time analysis, *Geogr. Res. Forum*, 31, 6–31.
- Guirguis, K., A. Gershunov, A. Tardy, and R. Basu (2014), The impact of recent heat waves on human health in California, *J. Appl. Meteorol. Climatol.*, 53(1), 3–19, doi:10.1175/JAMC-D-13-0130.1.
- Hilliker, J. L., and J. M. Fritsch (1999), An observations-based statistical system for warm-season hourly probabilistic forecasts of low ceiling at the San Francisco International Airport, *J. Appl. Meteorol.*, 38(12), 1692–1705.
- Iacobellis, S. F., and D. R. Cayan (2013), The variability of California summertime marine stratus: Impacts on surface air temperatures, *J. Geophys. Res. Atmos.*, 118, 9105–9122, doi:10.1002/jgrd.50652.
- Johnstone, J. A., and T. E. Dawson (2010), Climatic context and ecological implications of summer fog decline in the coast redwood region, *Proc. Natl. Acad. Sci. U.S.A.*, 107(10), 4533–4538.
- Klein, S. A., and D. L. Hartmann (1993), The seasonal cycle of low stratiform clouds, *J. Clim.*, 6(8), 1587–1606.
- Klein, S. A., D. L. Hartmann, and J. R. Norris (1995), On the relationships among low-cloud structure, sea surface temperature, and atmospheric circulation in the summertime northeast Pacific, *J. Clim.*, 8(5), 1140–1155.
- Kubar, T. L., D. E. Waliser, J. L. Li, and X. Jiang (2012), On the annual cycle, variability, and correlations of oceanic low-topped clouds with large-scale circulation using Aqua MODIS and ERA-Interim, *J. Clim.*, 25(18), 6152–6174, doi:10.1175/JCLI-D-11-00478.1.
- LaDochy, S., and M. Witiw (2012), The continued reduction in dense fog in the Southern California region: Possible causes, *Pure Appl. Geophys.*, 169(5–6), 1157–1163.
- Lilly, D. K. (1968), Models of cloud-topped mixed layers under strong inversions, *Q. J. Roy. Meteorol. Soc.*, 94, 292–309.
- Mantua, N. J., and S. R. Hare (2002), The Pacific Decadal Oscillation, *J. Oceanogr.*, 58(1), 35–44.
- Mantua, N. J., S. R. Hare, Y. Zhang, J. M. Wallace, and R. C. Francis (1997), A Pacific Interdecadal Climate Oscillation with impacts on salmon production, *Bull. Am. Meteorol. Soc.*, 78(6), 1069–1079.
- Mathiesen, P., J. M. Brown, and J. Kleissl (2012), Geostrophic wind dependent probabilistic irradiance forecasts for coastal California, *Sustainable Energy IEEE Trans.*, 4(2), 510–518.
- National Weather Service (2010), Aviation and synoptic observations, operations and services surface observing program (land), NWSPD 10–13, National Weather Service Instruction 10–1301. [Available online at <http://www.nws.noaa.gov/directives/sym/pd01013001curr.pdf>.]
- Norris, J. R. (1998a), Low cloud type over the ocean from surface observations. Part I: Relationship to surface meteorology and the vertical distribution of temperature and moisture, *J. Clim.*, 11, 369–382.
- Norris, J. R. (1998b), Low cloud type over the ocean from surface observations. Part II: Geographical and seasonal variations, *J. Clim.*, 11, 383–403.
- Norris, J. R., and C. B. Leovy (1994), Interannual variability in stratiform cloudiness and sea surface temperature, *J. Clim.*, 7, 1915–1925.
- Norris, J. R., Y. Zhang, and J. M. Wallace (1998), Role of low clouds in summertime atmosphere–ocean interactions over the North Pacific, *J. Clim.*, 11, 2482–2490.
- Overland, J., S. Rodionov, S. Minobe, and N. Bond (2008), North Pacific regime shifts: Definitions, issues and recent transitions, *Prog. Oceanogr.*, 77(2), 92–102.
- Pilié, R. J., E. J. Mack, C. W. Rogers, U. Katz, and W. C. Kocmond (1979), The formation of marine fog and the development of fog-stratus systems along the California coast, *J. Appl. Meteorol.*, 18(1), 1275–1286.
- Simon, R. L. (1977), The summertime stratus over the offshore waters of California, *Mon. Weather Rev.*, 105(10), 1310–1314.
- Williams, A. P., C. J. Still, D. T. Fischer, and S. W. Leavitt (2008), The influence of summertime fog and overcast clouds on the growth of a coastal Californian pine: A tree-ring study, *Oecologia*, 156(3), 601–611.
- Witiw, M. R., and S. LaDochy (2008), Trends in fog frequencies in the Los Angeles Basin, *Atmos. Res.*, 87(3), 293–300.
- Wood, R. (2012), Stratocumulus clouds, *Mon. Weather Rev.*, 140(8), 2373–2423, doi:10.1175/MWR-D-11-00121.1.
- Woodruff, S. D., et al. (2011), ICOADS Release 2.5: Extensions and enhancements to the surface marine meteorological archive, *Int. J. Climatol.*, 31(7), 951–967, doi:10.1002/joc.2103.



## Auxiliary Material

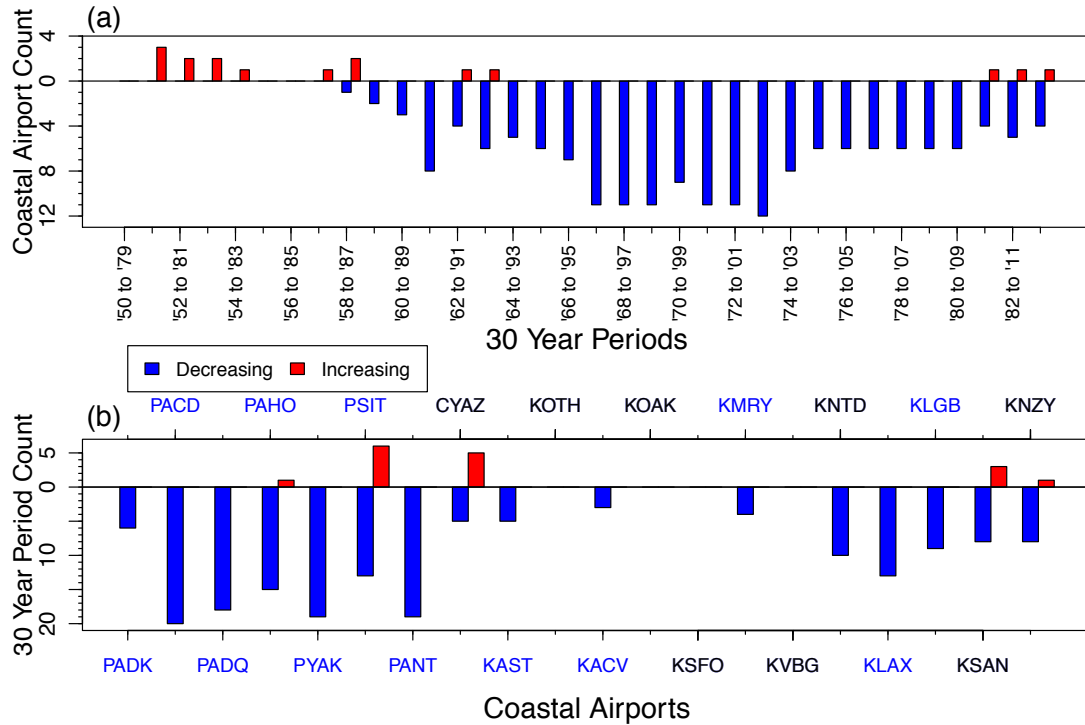


**Figure S1:** Significant decreasing (blue) and increasing (red) 30-year trends in CLC from a moving window analysis by time period (a) and by airport (b). There are 20 airports and 34 30-year periods from 1950 to 2012. CLC is significantly decreasing over the full 63 year record at airports labeled in blue.

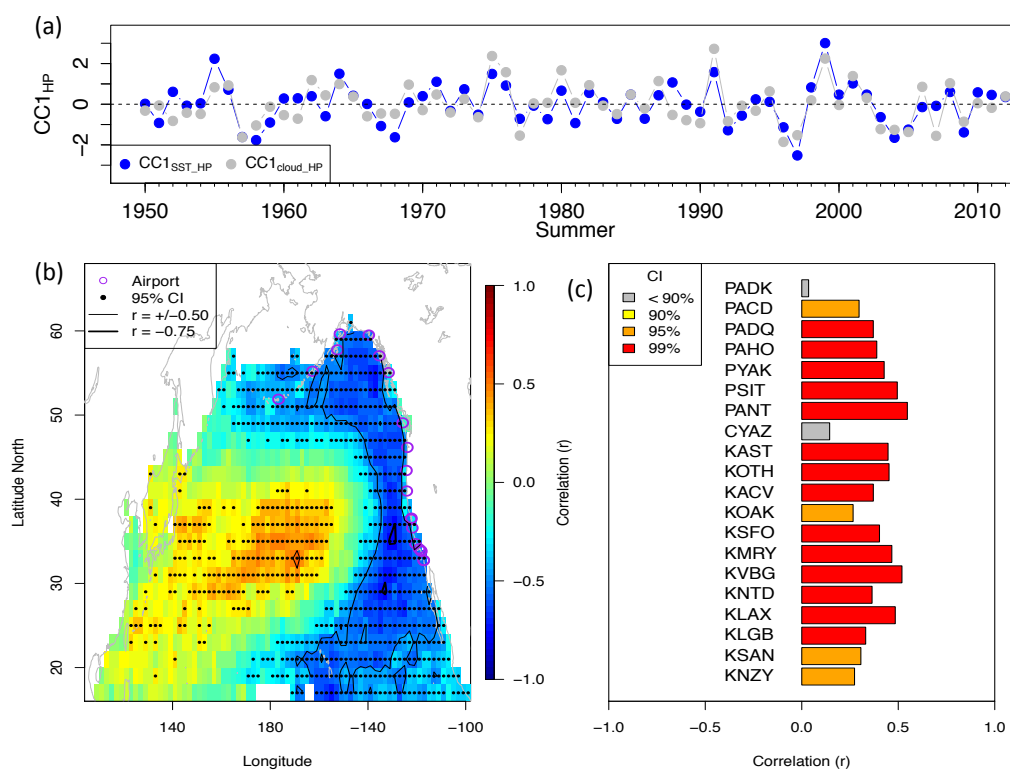


**Figure S2:** As in Figure3, but for high-pass filtered SST and CLC.

**Text S1:**

Radiosonde data is accessed from [esrl.noaa.gov/raobs](http://esrl.noaa.gov/raobs) for summers 1995 – 2012 at 0Z for seven coastal sites. Five sites (PACD, PADQ, PYAK, PANT, KOAK) are the same as those used for CLC and introduced in section 2.1. Additionally, Marine Corps Air Station Miramar, CA (KNKX) is about 15 miles northeast of KSAN, and Quillayute, WA (KUIL) is north of KAST and south of CYAZ and meant to represent this region. We identify subsidence inversion presence if there is increasing temperature (of at least 1°C ) with height over at least 100 m, and with inversion base above ground level and below 2,000 m.

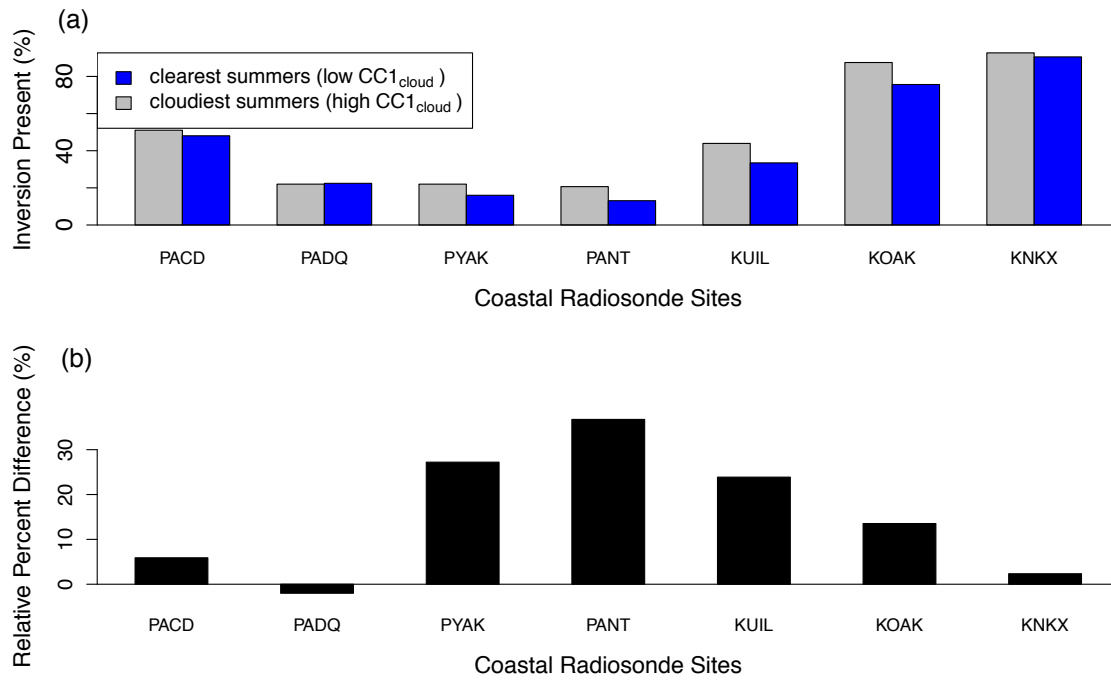


**Figure S3:** (a) Composite of inversion presence for clearest (cloudiest) summers as defined by the two lowest (highest)  $CC1_{cloud}$  values, over the overlapping radiosonde and CLC record, shown in blue (gray). (b) The relative difference between the gray and blue bars shown in (a).

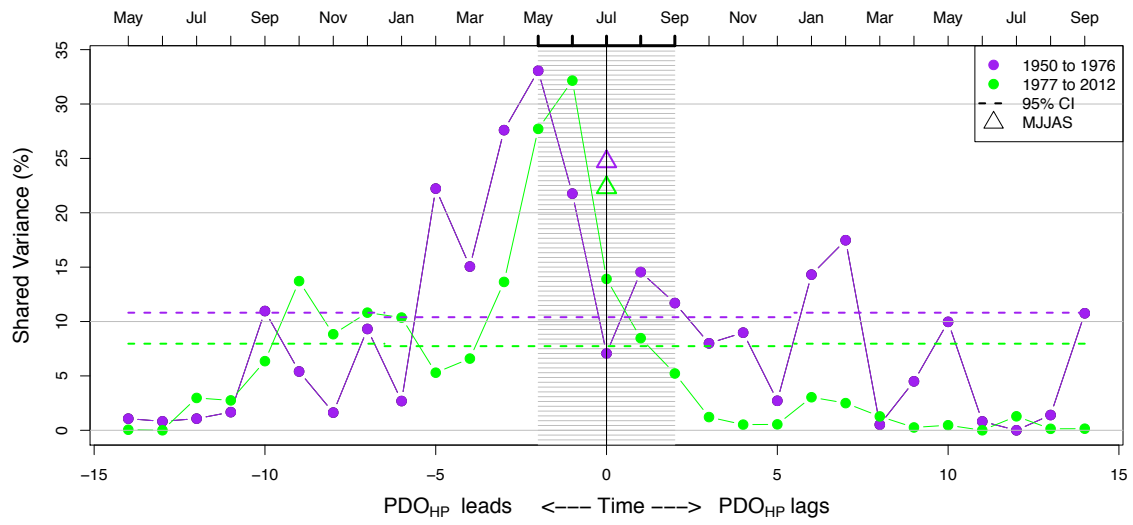


**Figure S4:** As in Figure 4, but for two separate time periods, 1950 to 1976 (purple) and 1977 to 2012 (green).